# *Chapter: 4*

## *Electric Field Induced Structural Phase Transformation in BMT-PT and BMZ-PT*

# Chapter-4

## 4.1 Introduction

In this chapter, we present the results of our investigation of electric field induced crystallographic phase transition in BMT-PT and BMZ-PT solid solutions across the morphotropic phase boundary. As discussed in chapter 3, for BMT-PT, morphotropic phase boundary exists around the composition x=0.37 and structure in the compositions range $0.33 \leq x \leq 0.40$ consists of coexisting monoclinic (space group Pm) and tetragonal (space group P4mm) phases [Upadhyay et al. (2015)]. The structure is predominantly tetragonal for the compositions with $x>0.40$. The compositions with $x<0.33$ are pseudocubic with short range monoclinic structure in the Pm space group [Upadhyay et al. (2015)]. Since piezoelectricity cannot be observed in ceramic samples unless they are poled, the ferroelectric ceramics are subjected to poling at high electric field to convert them into piezoelectric [Jaffe et al. (1971)]. It is therefore imperative to investigate electric field induced structural changes in these materials to get a better insight for development of new materials with superior electromechanical responses.

As discussed in chapter 3, in case of BMZ-PT, crystal structure is cubic with space group Pm3m for the compositions with $x<0.57$, tetragonal with space group P4mm for the compositions with $x>0.59$, and coexistence of cubic (space group Pm3m) and tetragonal (space group P4mm) phases for the intermediate compositions [Pandey et al. (2014)]. As will be discussed in subsequent sections, in BMZ-PT, after poling planar electromechanical coupling coefficient ($k_P$) is

observed for the cubic composition as well ($k_P$~0.21), which suggests possibility of an electric field induced phase transition in these compositions from paraelectric phase to ferroelectric phase under strong electric field [Pandey et al. (2014)]. The ferroelectrics with perovskite structure, have very close free energy landscape for pseudocubic/rhombohedral, orthorhombic, and tetragonal structures [Fu et al. (2000); Bell (2001)], and can transform from one phase to other via polarization rotation induced by externally applied electric field [Fu et al. (2000); Vanderbilt et al. (2001)]. The properties of piezoelectric solid solutions depend on the crystal structure, and the crystal structure is sensitive to external stimulus near MPB, an electric field induced phase transition is expected for the MPB compositions. Therefore a systematic electric field induced phase transition study is required for the BMZ-PT piezoceramics also to understand the physical phenomenon behind the phase transition and the origin of piezoelectric response in cubic compositions closed to MPB.

This Chapter presents the results of our investigation on electric field induced structural phase transformation in the BMT-PT and BZT-PT compositions across the morphotropic phase boundary.

## 4.2 Experimental details

The detailed sample preparation for BMT-PT and BMZ-PT are discussed in Chapter 2. For the investigation of electric field induced structural phase transformation, sintered pellets of BMT-PT and BMZ-PT were electroded by coating silver paste on flat surfaces and fired at 500$^o$C for 15 minutes. The fired-on silver paste was used for electroding of the pellets. The electroded pellets

were poled at 120$^{o}$C temperature in a silicon oil bath at DC electric fields of various strengths (10kV/cm, 20kV/cm, 30kV/cm, 40kV/cm and 50kV/cm). The electric field was removed after cooling the sample to the room temperature. To record the X-ray diffraction (XRD) data from poled samples, silver electrode was gently removed from one surface of the pellet. The XRD patterns of poled and unpoled samples of BMT-PT and BMZ-PT, were recorded at the scan rate of 2 degree/minute in the two-theta range 20$^{o}$-120$^{o}$ at the scan step of 0.02. The FullProf suite was used for Le-Bail profile matching structural analysis of the XRD data [Carvajal (2001), (2011)]. Due to domain evolution during poling the preferred orientation can leads to intensity mismatch between calculated and observed XRD pattern in the Rietveld fitting. Therefore, profile matching analysis was carried out by Le-bail refinement, which helps in overcoming the problem of preferred orientation during structural analysis. Background was modeled by sixth coefficient polynomial and pseudo-voigt function was used for modelling profile shape.

## 4.3 Electric field induced structural change in BMT-PT

### 4.3.1 Pseudocubic to monoclinic phase transition after poling in 0.68BMT-0.32PT

Fig.4.1 shows the selected (110), (111), and (200) pseudocubic XRD profiles for x=0.28 poled at 10kV/cm, 20kV/cm, 30kV/cm, and 50kV/cm along with the unpoled sample. As can be seen from Fig. 4.1, after poling the (200) profile transform into a clear doublet, the (111) pseudocubic profile also shows significantly enhanced broadening with a hump on lower two-theta side. The

broadening of the (110) profile is also significantly enhanced. Thus after poling the pseudocubic structure of the composition x=0.28 transforms to a clear low symmetry phase. To determine the structure of this phase resulting due to electric field induced phase transformation, we carried out Le-Bail full pattern matching analysis considering R3m, Cm, Pm space groups observed for low PT compositions in several MPB ceramics [Singh et al. (2003); Singh et al. (2006), (2007); Pandey et al. (2014)]. We find that it is the monoclinic structure with space group Pm which accounts most satisfactorily the observed diffraction pattern. Very good fit between observed and calculated profiles obtained by using monoclinic Pm space group for the sample poled at 30kV/cm is shown in Fig. 4.2. The refined lattice parameters for the unpoled and poled samples at 30kV/cm is given in Table 4.1. It is also evident from Fig. 4.1 that electric field induced phase transition is almost complete for field strength of 30kV/cm as there is no significant change in the XRD profile by increasing the field to 50kV/cm.

### 4.3.2 Structural changes in tetragonal compositions after poling in 0.62BMT-0.38PT

The selected (110), (111), and (200) pseudocubic XRD profiles for x=0.38 are shown in Fig. 4.3 for samples poled at various electric fields along with that for the unpoled sample. The structure of both the compositions are predominantly tetragonal in unpoled state as can be seen from the characteristic splitting of diffraction profiles shown in Fig. 4.3.

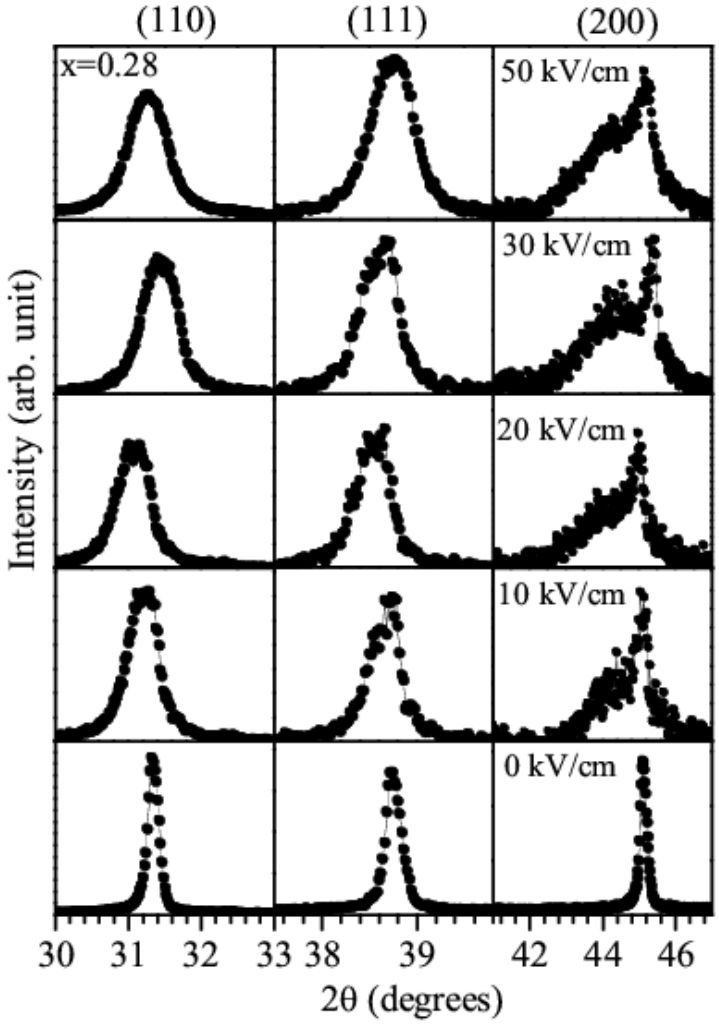


**Fig.4.1** Evolution of the pseudocubic (110), (111) and (200) XRD profile with varying the poling field strength for 0.72BMT-0.28PT ceramics.

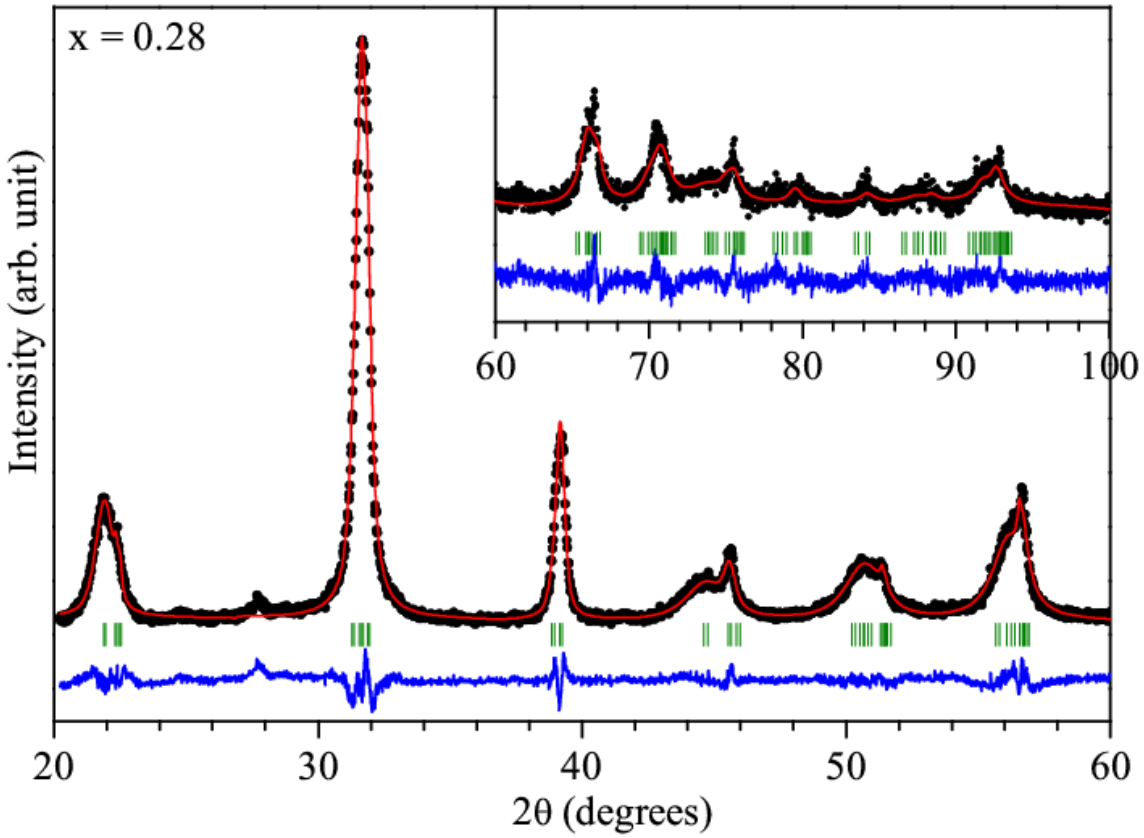


**Fig.4.2** Experimentally observed (dots), Rietveld calculated (continuous line) and their difference (continuous bottom line) profiles obtained after Le-Bail analysis for XRD data of 0.72BMT-0.28PT poled at 30kV/cm using monoclinic structure in the space group Pm. The vertical tick marks above the bottom line show peak positions.

As discussed in Chapter 3, section 3.5.3, the Rietveld analysis of the XRD data reveals small amount of coexisting monoclinic phase in Pm space group for these compositions. After poling most significant change is observed in (002) profile whose intensity is significantly enhanced in comparison to (200) profile. This may be ascribed to increased domain population along c-direction due to poling. A similar domain reorientation after poling is reported in tetragonal compositions of other MPB systems also [Ma et al. (2012); Daniels et al. (2009); Hinterstein et al. (2011); Schonau et al. (2007); Lalitha et al. (2014)]. The (111) pseudocubic profile is nearly unaffected after poling for x=0.38 in contrast to that for x=0.28. The pseudocubic (110) profile is a doublet with (101) and (110) reflections for tetragonal structure in unpoled state. After poling this doublet is not much affected. But a careful comparison of the profiles for samples poled at 30kV/cm with that for unpoled sample suggests that the intensity of the higher $2\theta$ side, (110) profile has decreased after poling. This is also ascribed to the domain reorientation after poling. It is clear from the foregoing that for the tetragonal compositions with x=0.38 there is no phase transition to a low symmetry phase after poling. The electric field poling only leads to domain reorientation after poling. Le-Bail full pattern matching analysis of the XRD pattern of the sample poled at 30kV/cm confirms a predominantly tetragonal structure with minority monoclinic (Pm) phase, similar to the unpoled sample. The full pattern Rietveld fit for the poled sample with x=0.38 is shown in Fig. 4.4, which is quite good. Table 4.1, compares the lattice parameters of the poled and unpoled samples. The c-parameter of the tetragonal phase shows significant elongation after poling.

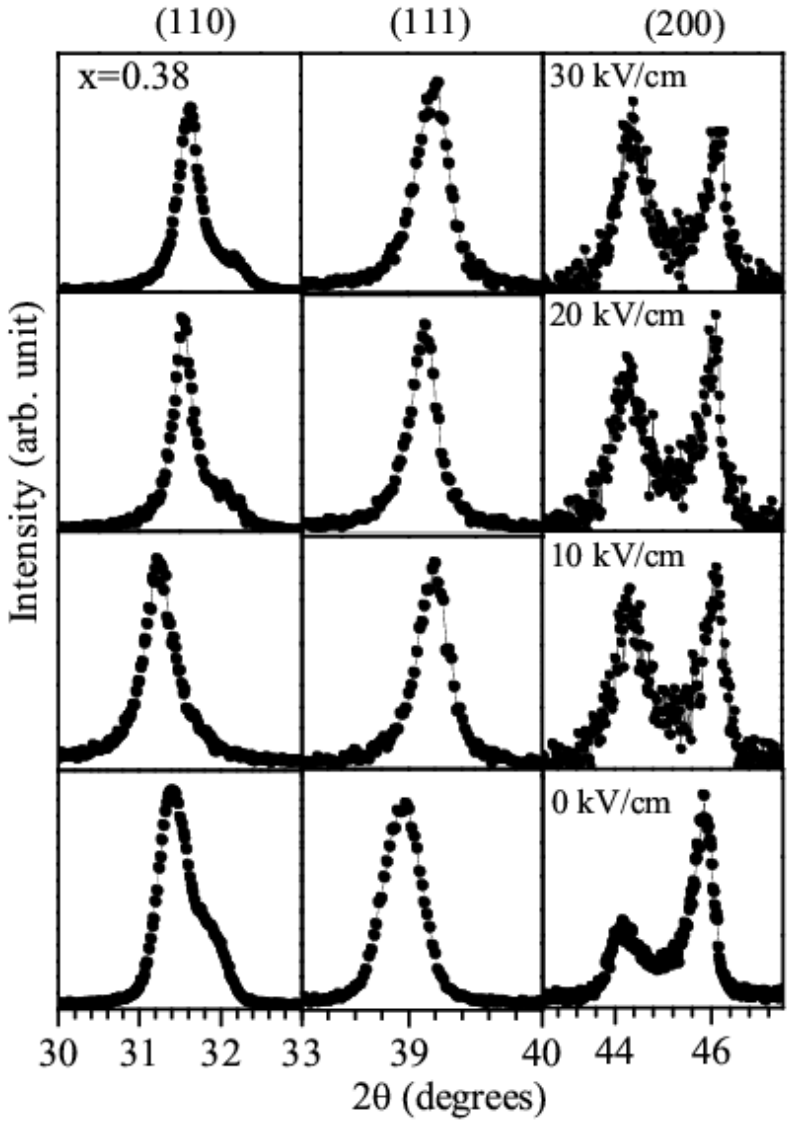


**Fig.4.3** Evolution of the pseudocubic (110), (111) and (200) XRD profile with varying the poling field strength for 0.62BMT-0.38PT ceramics.

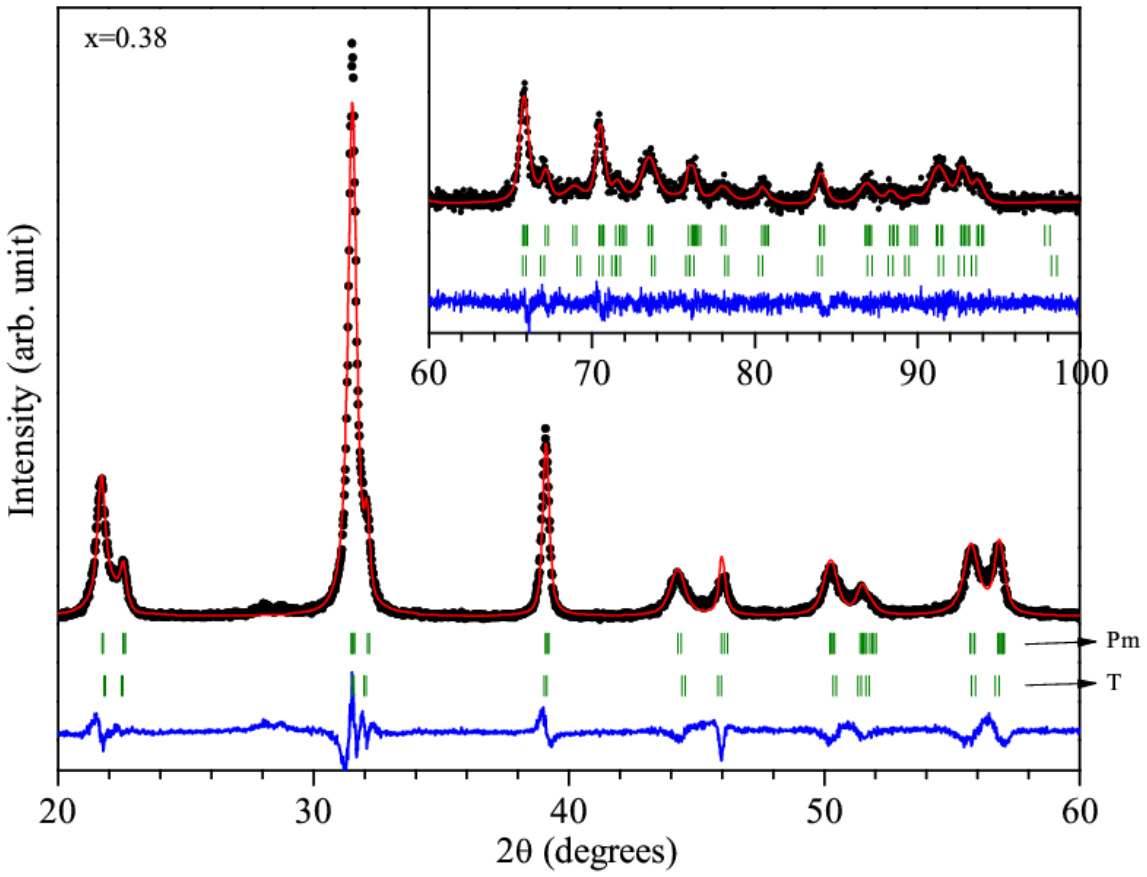


**Fig.4.4** Experimentally observed (dots), Rietveld calculated (continuous line) and their difference (continuous bottom line) profiles obtained after Le-Bail analysis of XRD data for 0.62BMT-0.38PT poled at 30kV/cm using coexisting monoclinic and tetragonal structures with space groups Pm+P4mm. The vertical tick marks above the bottom line show peak positions.

### 4.3.3 Structural changes in MPB composition after poling in 0.65BMT-0.35PT

Fig. 4.5 shows the selected (110), (111), and (200) pseudocubic XRD profiles for x=0.35 poled at 10kV/cm, 20kV/cm, and 30kV/cm along with the unpoled sample. As can be seen from Fig. 4.5, the XRD profiles of the unpoled sample has the asymmetric tails on higher and lower 2θ sides for the (110) and (200) profiles. The triplet nature of the (200) and (110) profiles confirms the coexistence of tetragonal structure with a low symmetry phase. As discussed in chapter 3, the Rietveld analysis of the XRD data reveals that the structure of the composition with x=0.35 is predominantly monoclinic with small amount of coexisting tetragonal phase in P4mm space group [Upadhyay et al. (2015)]. The XRD peaks corresponding to the tetragonal and monoclinic phases are marked by 'T' and 'M' respectively in Fig. 4.5 for the unpoled sample. After poling the (200) profile is drastically modified with the appearance of a well resolved doublet and a long tail on the lower two-theta side. This suggests that pseudocubic monoclinic (Pm) phase undergoes an electric field induced phase transformation to long ranged monoclinic structure with more prominent splitting in the XRD profiles similar to that observed for the composition with x=0.28. Further the tetragonal phase is undergoing a domain reorientation after electric field poling similar to that observed for the compositions with x=0.38. Similar to the composition with x=0.28, the (111) profile has got significant broadening after poling with asymmetry on the lower two-theta side. The overlapping of tetragonal and monoclinic profiles leads to very broad peak for (110) pseudocubic XRD profile after poling. Full pattern Le-Bail profile fit for the sample poled at 30kV/cm is shown in Fig. 4.6 using coexisting tetragonal and monoclinic structures. The fit is quite good. Table 4.1 compares the lattice parameters of the unpoled and poled samples. The c- parameter of tetragonal structure shows significant elongation after poling.

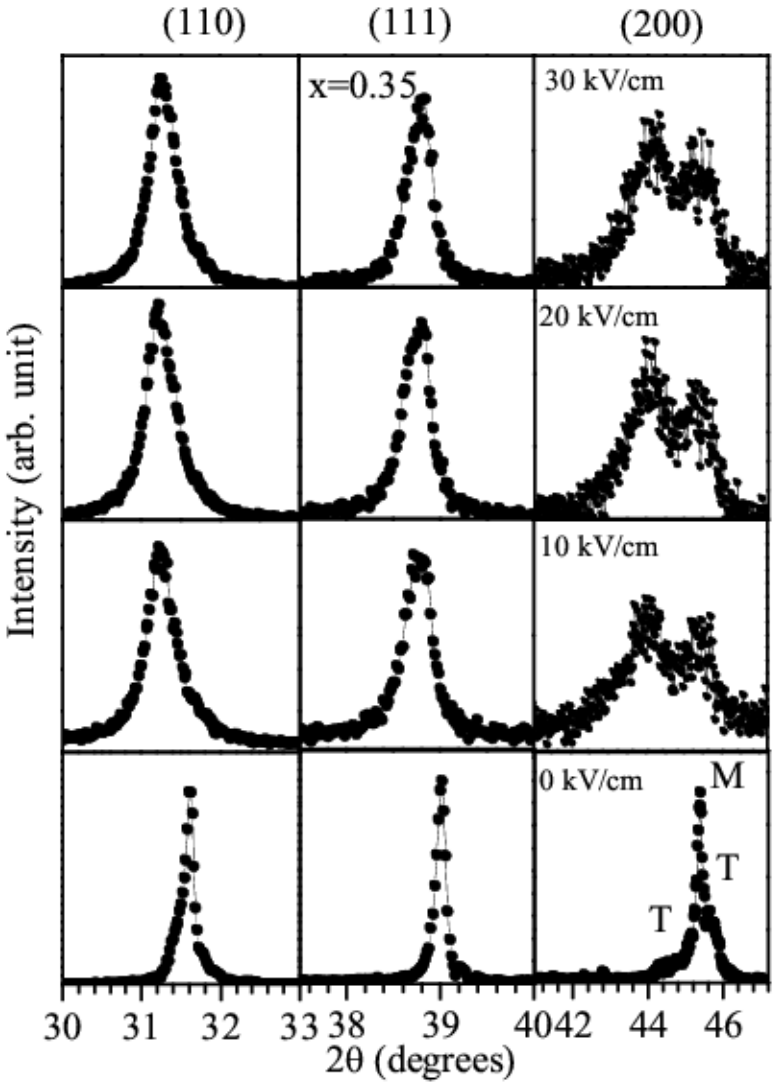


**Fig.4.5** Evolution of the pseudocubic (110), (111) and (200) XRD profile with varying poling field strength for 0.65BMT-0.35PT ceramics.

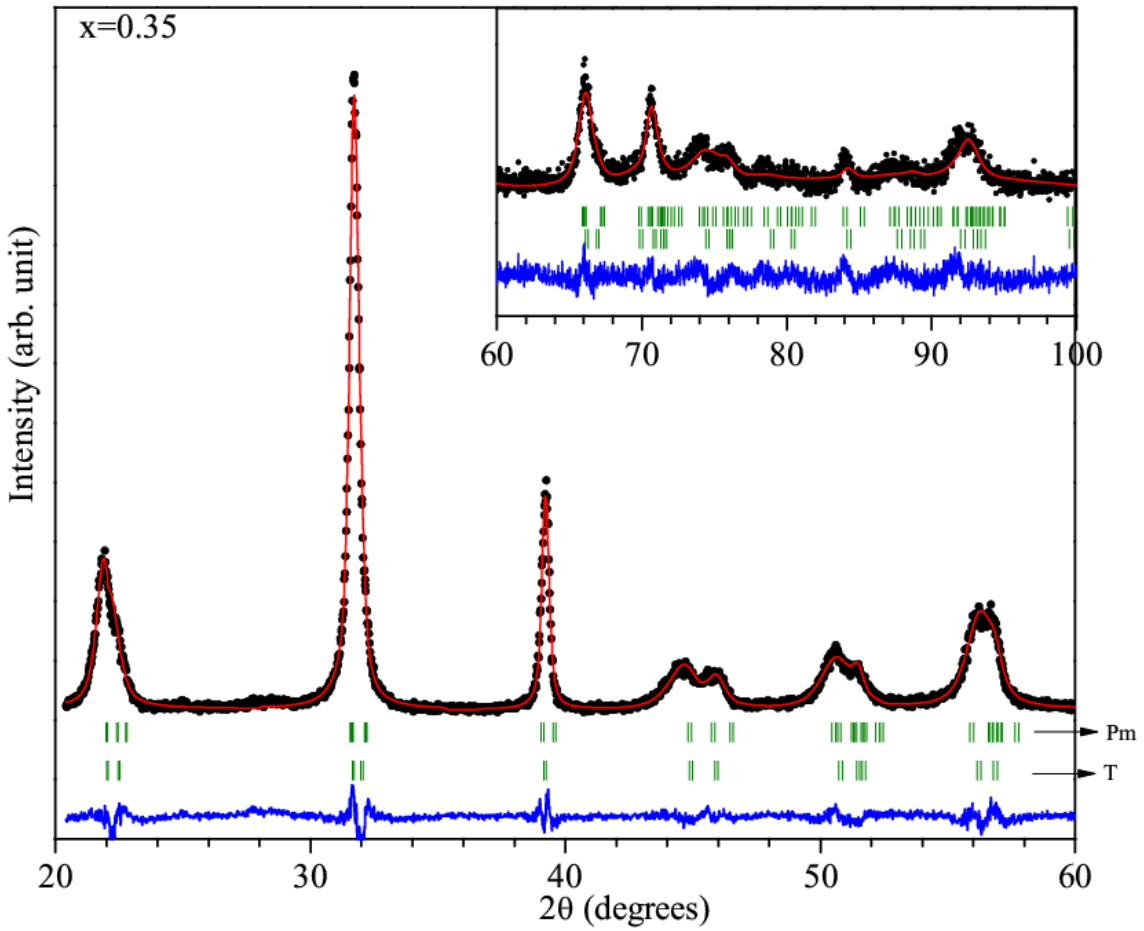


**Fig.4.6** Experimentally observed (dots), Rietveld calculated (continuous line) and their difference (continuous bottom line) profiles obtained after Le-Bail analysis of XRD data for 0.65BMT-0.35PT using coexisting monoclinic and tetragonal structures with space groups Pm+P4mm. The vertical tick marks above the bottom line show peak positions.

**Table 4.1:** Refined Lattice parameters obtained by Rietveld profile matching analysis for the poled 30kV/cm and unpoled sample of (1-x)$Bi(Mg_{1/2}Ti_{1/2})O_3$-x$PbTiO_3$ piezoceramics using monoclinic (Pm) and tetragonal (P4mm) structures.

| (x) | Space group | Lattice parameters (Å) (**poled**) | Lattice parameters (Å) (**unpoled**) |
|---|---|---|---|
| 0.28 | Pm | a=4.0051(9), b=3.9877(9) c=4.049(1), β=90.087(9)$^o$ | a=3.9813(3), b=3.975(2) c=3.9880(6), β=90.074(2)$^o$ |
| 0.38 | Pm | a=3.9783(1), b=3.9631(5) c=4.0196(7), β=90.078(1)$^o$ | a=3.9801(2), b=3.969(6) c=4.0068(3), β=90.346(3)$^o$ |
| 0.38 | P4mm | a=3.9552(4), c=4.0877(6) | a=3.9403(5), c=4.0808(3) |
| 0.35 | Pm | a=3.9713(5), b=3.9641(2) c=4.016(5), β=90.072(3)$^o$ | a=3.9801(9), b=3.9675(4) c=4.0026(6), β=90.232(2)$^o$ |
| 0.35 | P4mm | a=3.9642(7), c=4.0871(6) | a=3.9465(5), c=4.0688(2) |

### 4.3.4 Polarization (P) - Electric field (E) hysteresis loop studies for BMT-PT

In Fig. 4.7 we show the polarization (P) – electric (E) field hysteresis loops for the unpoled BMT-PT samples with compositions x = 0.28, 0.35, 0.38, and 0.40. As can be seen from Fig. 4.7 the hysteresis loops are not saturated. Further, hysteresis loop is more open for lower PT compositions than for higher compositions. The maximum remnant Polarization (Pr) is obtained for the composition with x=0.28 having pseudocubic structure. Pr is minimum for the composition with x=0.40. Snell et al. (2005) also reported similar results and did not get the saturated loop in unpoled samples of BMT-PT.

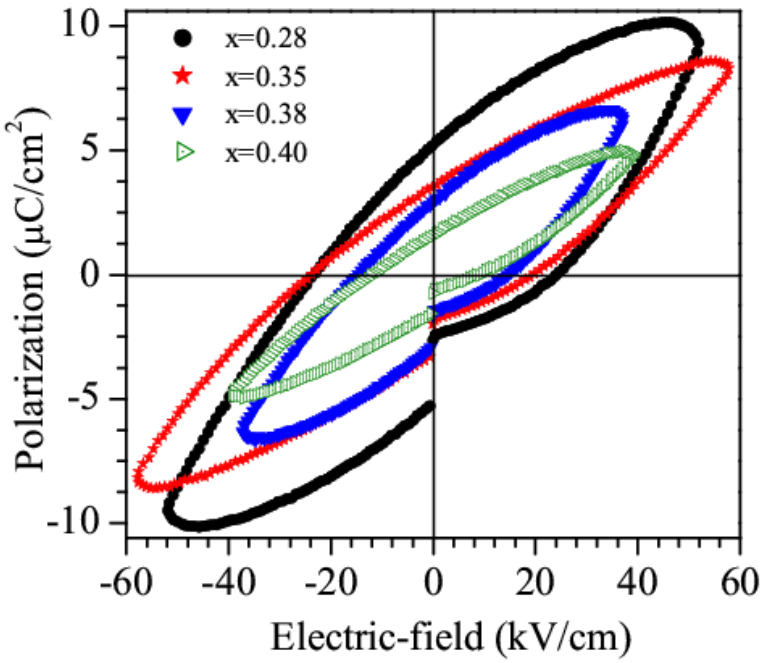


**Fig.4.7** Polarization (P) – Electric (E) field hysteresis loops for the unpoled samples of (1-x)Bi($Mg_{1/2}Ti_{1/2}$)$O_3$-x$PbTiO_3$ ceramics with x=0.28, 0.35, 0.38, and 0.40.

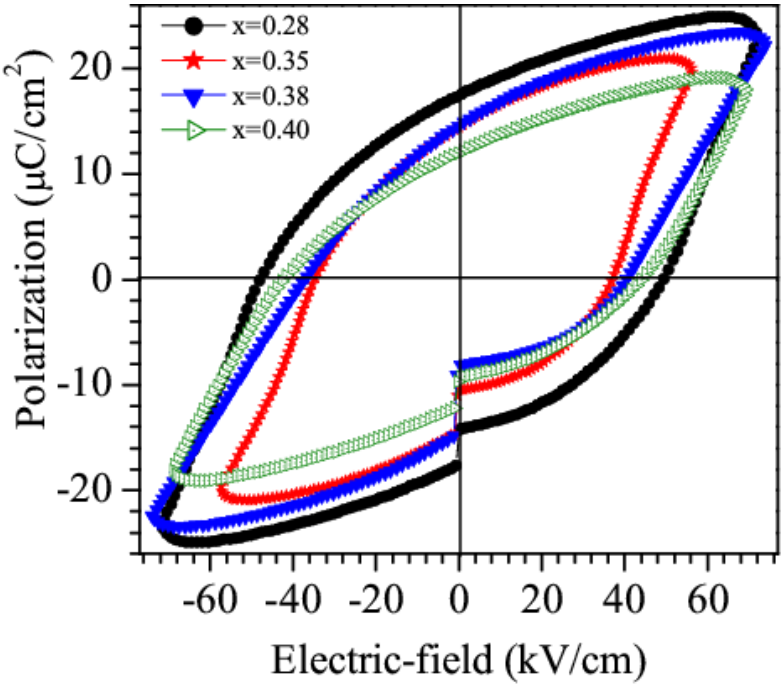


**Fig.4.8** Polarization (P) – Electric (E) field hysteresis loops for the (1-x)Bi($Mg_{1/2}Ti_{1/2}$)$O_3$-x$PbTiO_3$ ceramics with x=0.28, 0.35, 0.38, and 0.40 poled at 30 kV/cm.

The hysteresis loops open and become saturated clearly like ferroelectric hysteresis loop after poling as shown in Fig. 4.8. Maximum value of remnant polarization (Pr) is obtained for the pseudocubic composition with x=0.28, while Pr is minimum for x=0.40. The 'Pr' is comparable for the compositions with x=0.35 and 0.38. Since the composition with x=0.28 transform to monoclinic phase in Pm space group after poling, presence of monoclinic phase may be attributed to largest 'Pr' for this composition. In a monoclinic phase with space group Pm the polarization vector has more freedom to rotate in (010) plane in response to applied electric field in comparison to the tetragonal phase where it is confined to '6' fixed <001> crystallographic directions along which it can orient. With increasing PT concentration there is appearance of coexisting tetragonal phase which may be attributed to lower polarization at higher PT concentration. As reported by Randall et al. (2004) and Zhang et al. (2010) the BMT-PT ceramic undergoes relaxor like diffuse phase transition at higher temperatures. Presence of $Mg^{+2}/Ti^{+4}$ ions at B-site and $Bi^{+3}/Pb^{+2}$ ions at A-site introduce ionic size and charge disorders at A and B sites. These disorders generate random fields [Pirc et al. (1999) and Westphal et al. (1992)] in the lattice which may prevent development of long range ferroelectric order and appearance of saturated hysteresis loops in unpoled samples. After poling the random fields are suppressed by external electric field and the structure of composition with x=0.28 changes to a long ranged monoclinic phase due to co-operative movement of the ions leading to long range ferroelectric order and appearance of well saturated hysteresis loops. In future it will be interesting to investigate the domain structure

of various compositions of BMT-PT across MPB both in poled and unpoled state to develop a better understanding of the phenomenon.

## 4.4 Electric field induced structural changes in BMZ-PT

Fig. 4.9 shows the variation of the planar electromechanical coupling coefficient ($k_P$) with composition for BMZ-PT ceramics. The value of $k_P$ is significantly lower (~0.26) than for widely used MPB systems such as PZT and PMN-PT. As reported by Fu and Cohen (2000), the high piezoelectric response near the MPB is linked to the ease of rotation of the polarization vector under external stimuli such as electric field or stress. The presence of monoclinic phase in the MPB region provides a lower-energy path for the rotation of the polarization vector. This is the reason why Bi-based MPB systems such as BS-PT also exhibit a high piezoelectric response for the MPB compositions [Eitel et al. (2001), (2002); Chaigneau et al. (2007); Alguero et al. (2012)]. The presence of a cubic phase coexisting with the tetragonal phase in the BMZ-PT system may be attributed to lower $k_P$ as compared with PZT [Park et al. (1997); Noheda et al. (1999)], PMN-PT [Park et al. (1997); Singh et al. (2003), (2006)] and BS-PT [Eitel et al. (2001), (2002); Chaigneau et al. (2007); Alguero et al. (2012)]. The electromechanical coupling coefficient $k_P$ (~0.21) is obtained for the cubic composition with x=0.55, which is not expected for the centrosymmetric structure. This could be explained only if there is an electric-field induced phase transition from a paraelectric cubic phase to a ferroelectric phase with non-centrosymmetric structure.

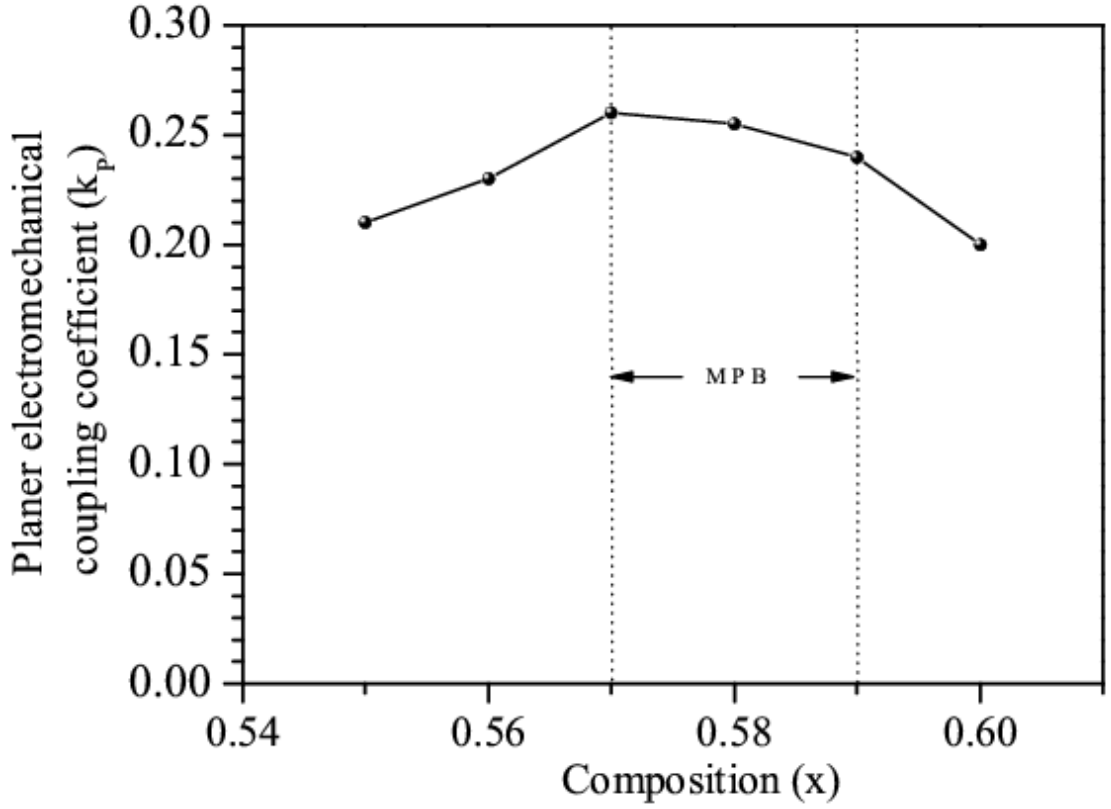


**Fig.4.9** Variation in the electromechanical coupling coefficient ($k_P$) with composition for (1-x)Bi($Mg_{1/2}Zr_{1/2}$)$O_3$-x$PbTiO_3$ ceramics. The continuous line is a visual guide.

### 4.4.1 Cubic to tetragonal phase transition after poling in 0.45BMZ-0.55PT

To discuss the structural changes as a function of poling field we show in Fig. 4.10 the selected (111), (200) and (220) pseudocubic XRD profiles for BMZ-PT piezoceramics for the composition with x=0.55 poled at 10kV/cm, 20kV/cm, 30kV/cm and 40kV/cm along with the unpoled sample. As can be seen from Fig. 4.10 with increasing poling field the peak broadening of (200) profile increases and convert into a clear doublet for an electric field strength of 30kV/cm. Further on increasing the field to 40kV/cm no significant change is observed for (200) profile. The width of the pseudocubic (220) profile also shows enhanced broadening after poling. There is no significant change observed in pseudocubic (111) profile. Clear splitting of (200) profile after poling confirms an electric field induced phase transition in this composition. Full pattern profile matching analyse was carried out to analysis the structure of poled samples. We find that after poling the cubic structure of the composition x=0.55 transforms into coexistence of the two phases with cubic (space group Pm3m) and tetragonal (space group P4mm) structures. The Le-Bail full pattern matching fit of the XRD pattern of the sample poled at 30kV/cm is shown in Fig. 4.11. Very good fit between observed and Rietveld calculated XRD profiles is obtained by using coexisting cubic (space group Pm3m) and tetragonal (space group P4mm) structures.

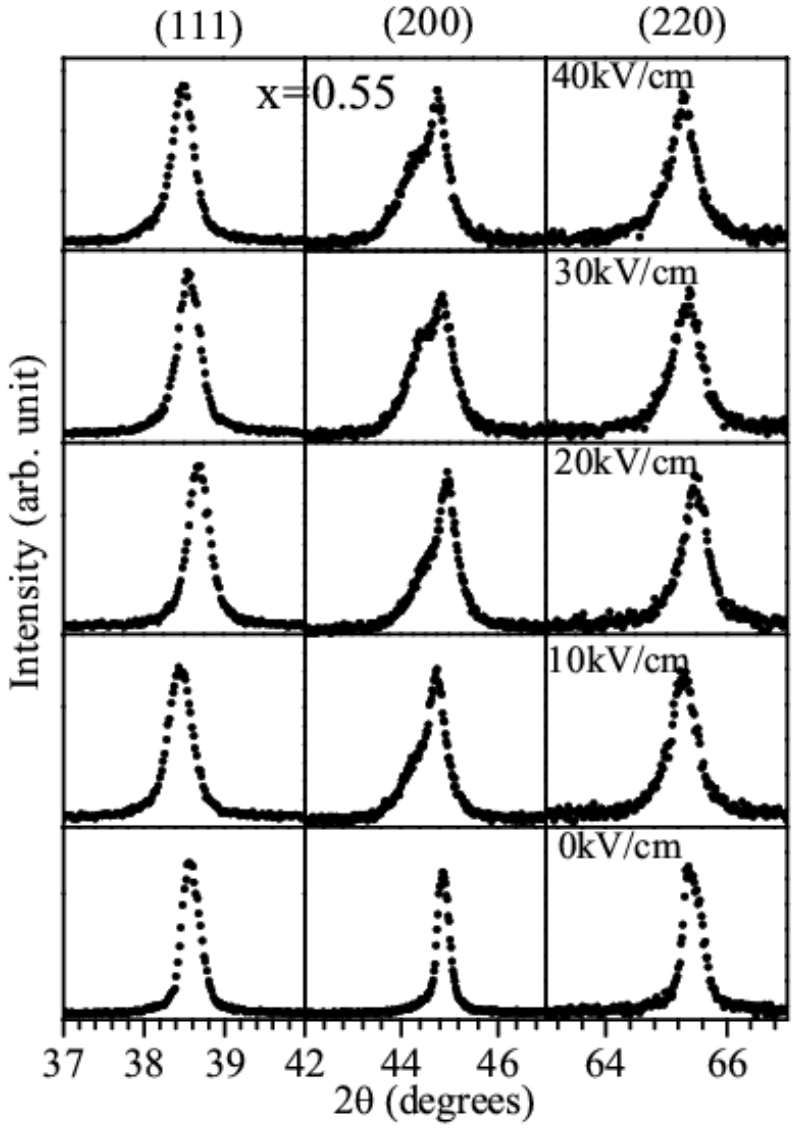


**Fig.4.10** Evolution of the pseudocubic (111), (200) and (220) XRD profile with varying poling field strength for 0.45BMZ-0.55PT ceramics.

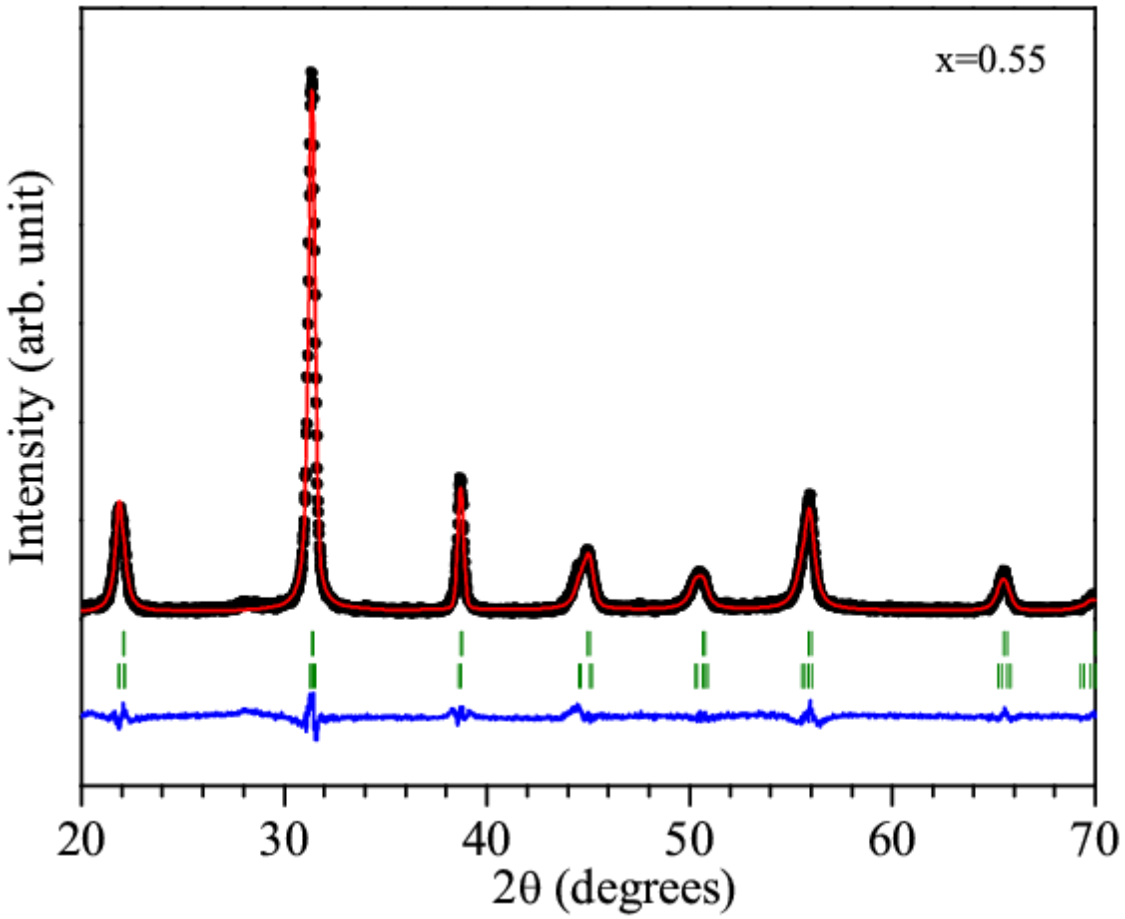


**Fig.4.11** Experimentally observed (dots), Rietveld calculated (continuous line) and their difference (continuous bottom line) profiles obtained after Le-Bail analysis of XRD data for 0.45BMZ-0.55PT. The vertical tick marks above the bottom line show peak positions.

### 4.4.2 Structural changes in tetragonal composition after poling (0.39BMT-0.61PT)

The selected (111), (200) and (220) pseudocubic XRD profiles in BMZ-PT for the composition with x=0.61 poled at 10kV/cm, 20kV/cm, and 30kV/cm along with the unpoled sample are shown in Fig. 4.12. After poling no new reflection appears. This suggest that structure remains tetragonal for poled samples. As can be seen from Fig. 4.12 with increasing the poling field the intensity of the (002) XRD profile is significantly enhanced in comparison to the intensity of (200) profile. Further, the (002) profile is seen to be shifted towards lower angle side at high poling field. Also we observe significant diminution in the intensity of (220) profile in comparison to the (202) profile. This suggests that the domain extension and reorientation takes place during electric field poling. Poling leads to domain reorientation/elongation along c-axis. There is no significant change for the pseudocubic (111) profile after poling. The Le-Bail full pattern profile matching fit using tetragonal structure (space group P4mm) for sample poled at 30kV/cm is shown in Fig. 4.13, which is quite good fit.

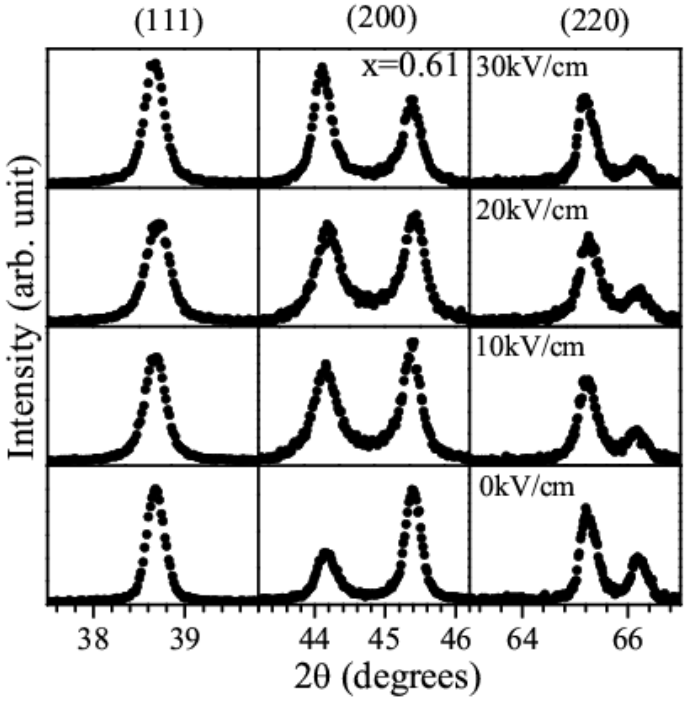


**Fig.4.12** Evolution of the pseudocubic (111), (200) and (220) XRD profile with varying poling field strength for 0.39BMZ-0.61PT ceramics.

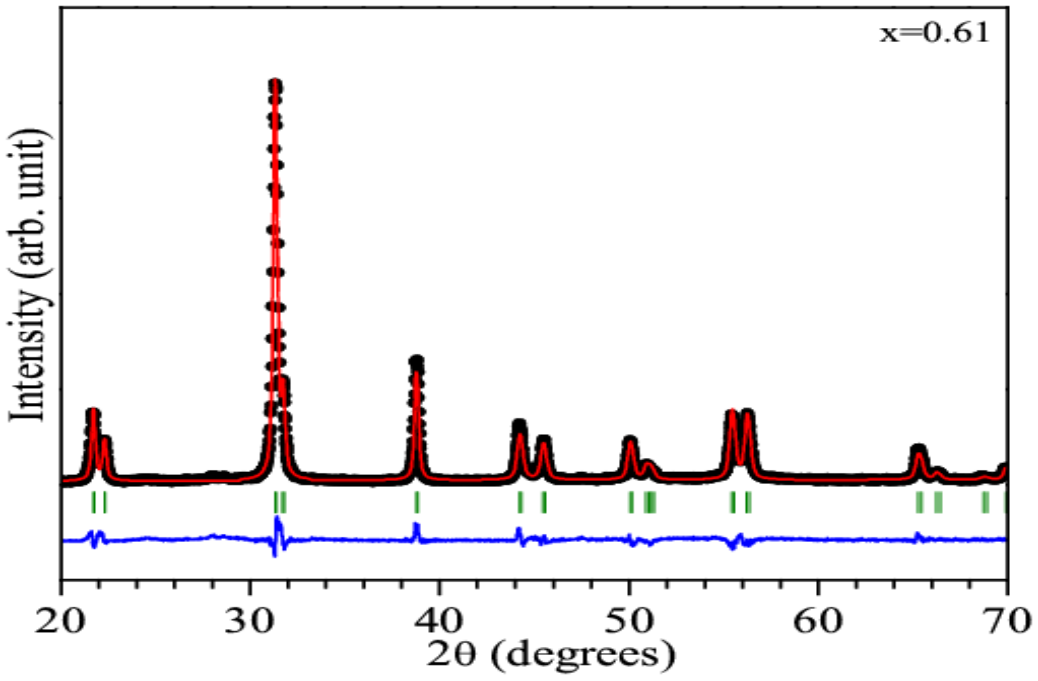


**Fig.4.13** Experimentally observed (dots), Rietveld calculated (continuous line) and their difference (continuous bottom line) profiles obtained after Le-Bail analysis of XRD data for 0.39BMZ-0.61PT. The vertical tick marks above the bottom line show peak positions.

### 4.4.3. Structural phase transition in MPB composition after poling (0.42BMZ-0.58PT)

The selected (111), (200), and (220) pseudocubic XRD profiles of BMZ-PT for the composition with x=0.58 poled at 10kV/cm, 20kV/cm, and 30kV/cm along with the unpoled sample are shown in Fig. 4.14. As discussed in chapter 3, for the unpoled sample, coexistence of the two phases is observed as revealed from the triplet nature of the (200) and (220) profiles. The structure of virgin sample of the composition with x=0.58 is coexistence of cubic (space group Pm3m) and tetragonal phases in P4mm space group [Pandey et al. (2014)]. After electric field poling, as can be seen from Fig. 4.14, a drastic modification in the intensity of the (002) profile occurs. As we increase the poling field strength, the intensity of (002) and (200) profiles of the tetragonal phase are enhanced, while (200) profile of cubic phase shows reducing trend. A clear doublet in (002)/(200) profiles is observed for the poling field strength of 30kV/cm. The (220) profile also changes with the poling field. The broadening of the (220) peak is increased after poling. We did not observe much change in (111) profile. The Rietveld full pattern matching analysis was done to determine the structure of poled sample considering various plausible structure. Our analysis confirms that the structure of poled samples is also coexistence of cubic and tetragonal phases similar to unpoled sample. The full pattern Le-Bail profile matching fit with coexistence of cubic (space group Pm3m) and tetragonal (space group P4mm) phases for the sample poled at 30kV/cm is shown in Fig. 4.15. The fit is quite satisfactory.

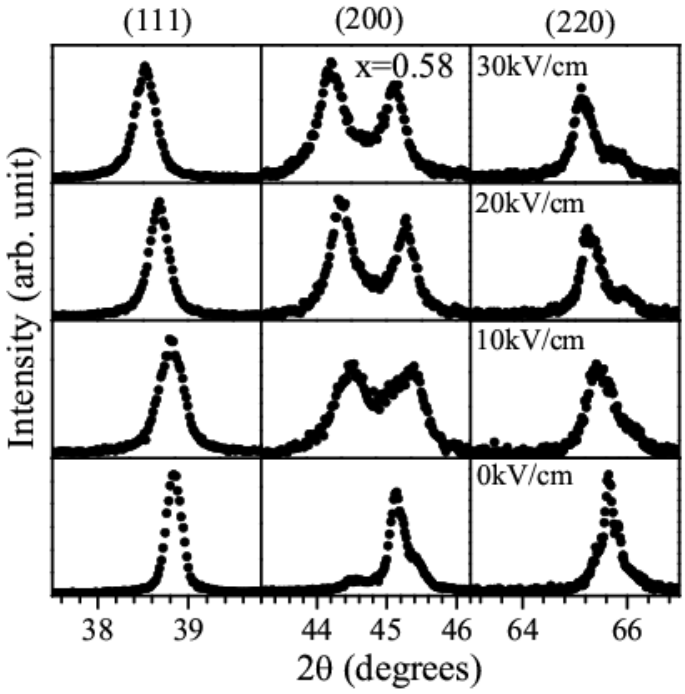


**Fig.4.14** Evolution of the pseudocubic (110), (200) and (220) XRD profile with varying poling field strength for 0.42BMZ-0.58PT ceramics.

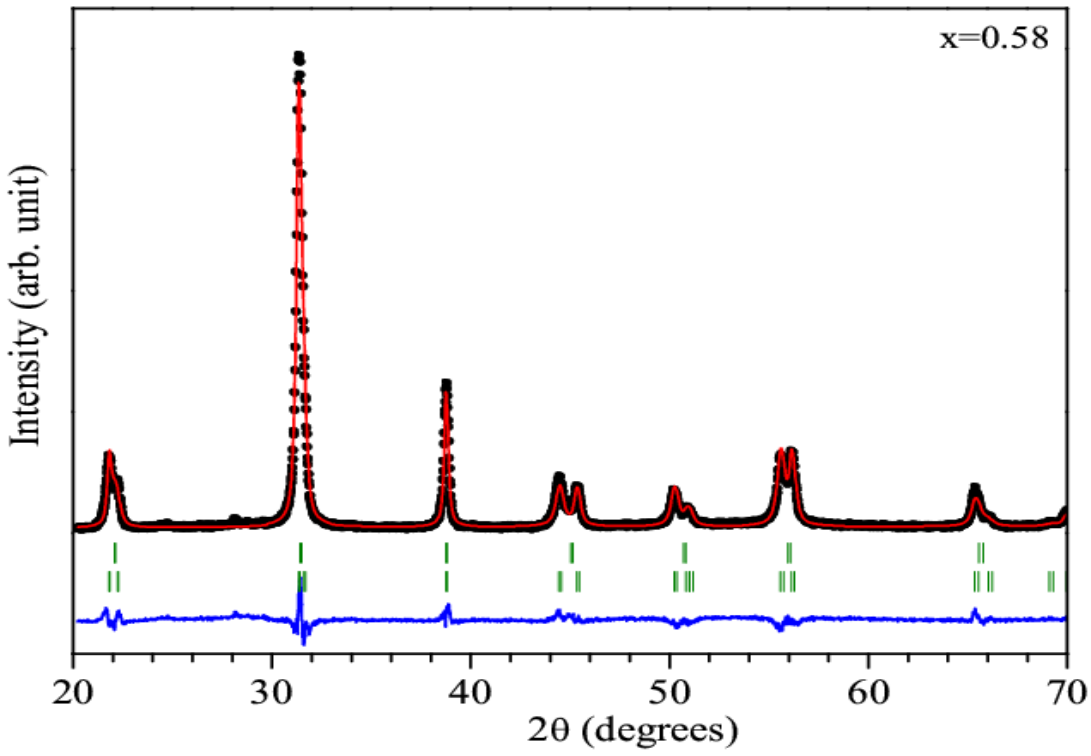


**Fig.4.15** Experimentally observed (dots), Rietveld calculated (continuous line) and their difference (continuous bottom line) profiles obtained after Le-Bail analysis of XRD data for 0.42BMZ-0.58PT. The vertical tick marks above the bottom line show peak positions.

### 4.4.4 Modifications in the lattice parameters after poling

The variation of lattice parameters with composition of BMZ-PT piezoceramics with x=0.55, 0.58, and 0.61 poled at electric field of 30kV/cm along with the unpoled sample is shown in Fig. 4.16. The cubic lattice parameters for unpoled and poled sampled are denoted by $a_C$ and $a_{C\_P}$ respectively. The tetragonal lattice parameters of the unpoled samples are denoted by $a_T$ and $c_T$ and for samples poled at electric field 30kV/cm are denoted by $a_{T\_P}$ and $c_{T\_P}$. As can be seen from Fig. 4.16 there is no significant change in the lattice parameters for the composition x=0.61, which is tetragonal in unpoled state. The tetragonality of the tetragonal phase in the MPB composition is significantly increased after poling. The tetragonality of the phase resulting from the electric field induced phase transition in x=0.55 is lower than the other two compositions. This suggest that the tetragonal composition (x=0.61) undergoes mostly domain reorientation after electric field poling, while tetragonal phase of unpoled MPB composition undergoes significant domain extension and reorientation along c-axis.

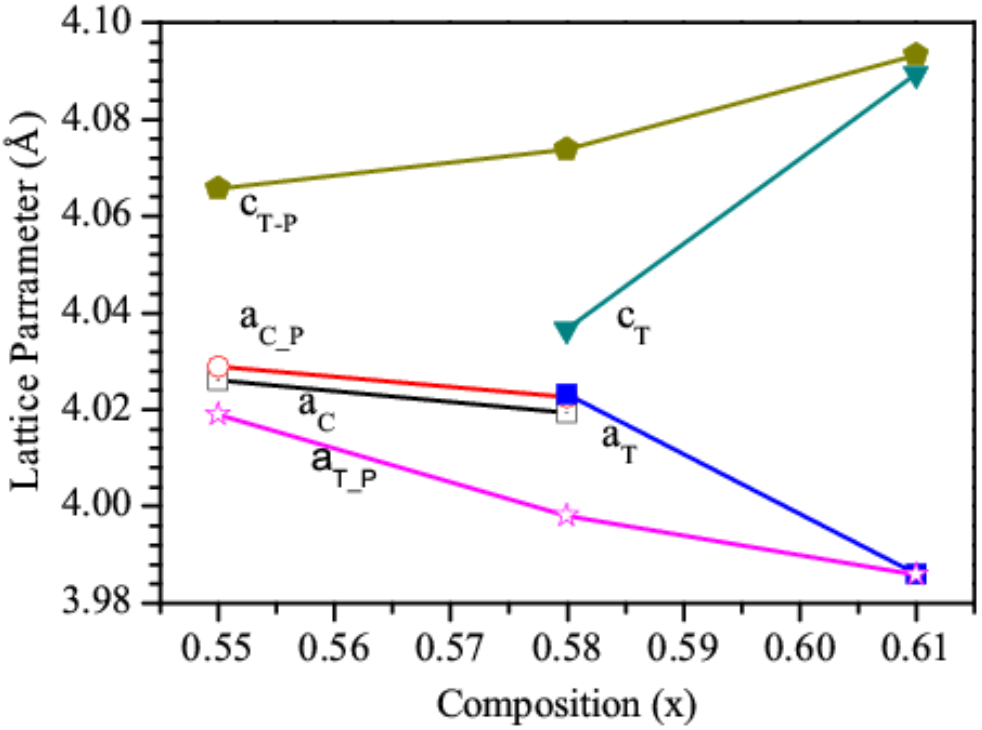


**Fig.4.16** Variation of lattice parameter with composition (x) of BMZ-PT piezoceramics poled at an electric field 30kV/cm along with the unpoled sample.

### 4.4.5 Polarization (P) – Electric field (E) hysteresis loop studies for BMZ-PT

Polarization (P) - electric field (E) hysteresis loops for the compositions with x=0.56 (cubic), 0.58 (cubic+tetragonal) and x=0.60 (tetragonal) are shown in Fig. 4.17 (a)-(c), respectively. As can be seen from Fig. 4.17, a well-saturated hysteresis loop is observed for x=0.56. Since the structure of this composition is cubic at room temperature, the hysteresis loop should not be obtained if it is the centrosymmetric paraelectric phase. This anomalous result could be explained only if we consider the presence of the relaxor behavior in this composition. In fact, temperature dependence of the dielectric permittivity of BMZ-PT with x=0.55 reported by Suchomel and Davies (2004) exhibits a strong peak at ~250$^{o}$C ($T_m'$) with large frequency dispersion suggesting the presence of strong relaxor features. Recently in the case of $Pb(Mg_{1/3}Nb_{2/3})O_3$ (PMN) [Fu et al. (2009)], it has been reported that a well-saturated hysteresis loop similar to that of normal ferroelectrics is observed when the temperature is lowered below the freezing temperature ($T_{vf}$=220K) [Colla et al. (1995); Viehland et al. (1991)]. The appearance of well-saturated hysteresis loop for x=0.55 mislead Shabbir et al. (2007) and Qureshi et al. (2007) into drawing the conclusion that this composition is rhombohedral, even though no splitting was observed in the XRD profiles. More surprisingly, the hysteresis loops shown in Fig. 4.17c for the tetragonal phase with x=0.60 are very slim in comparison to that for x=0.56 and saturation is not reached.

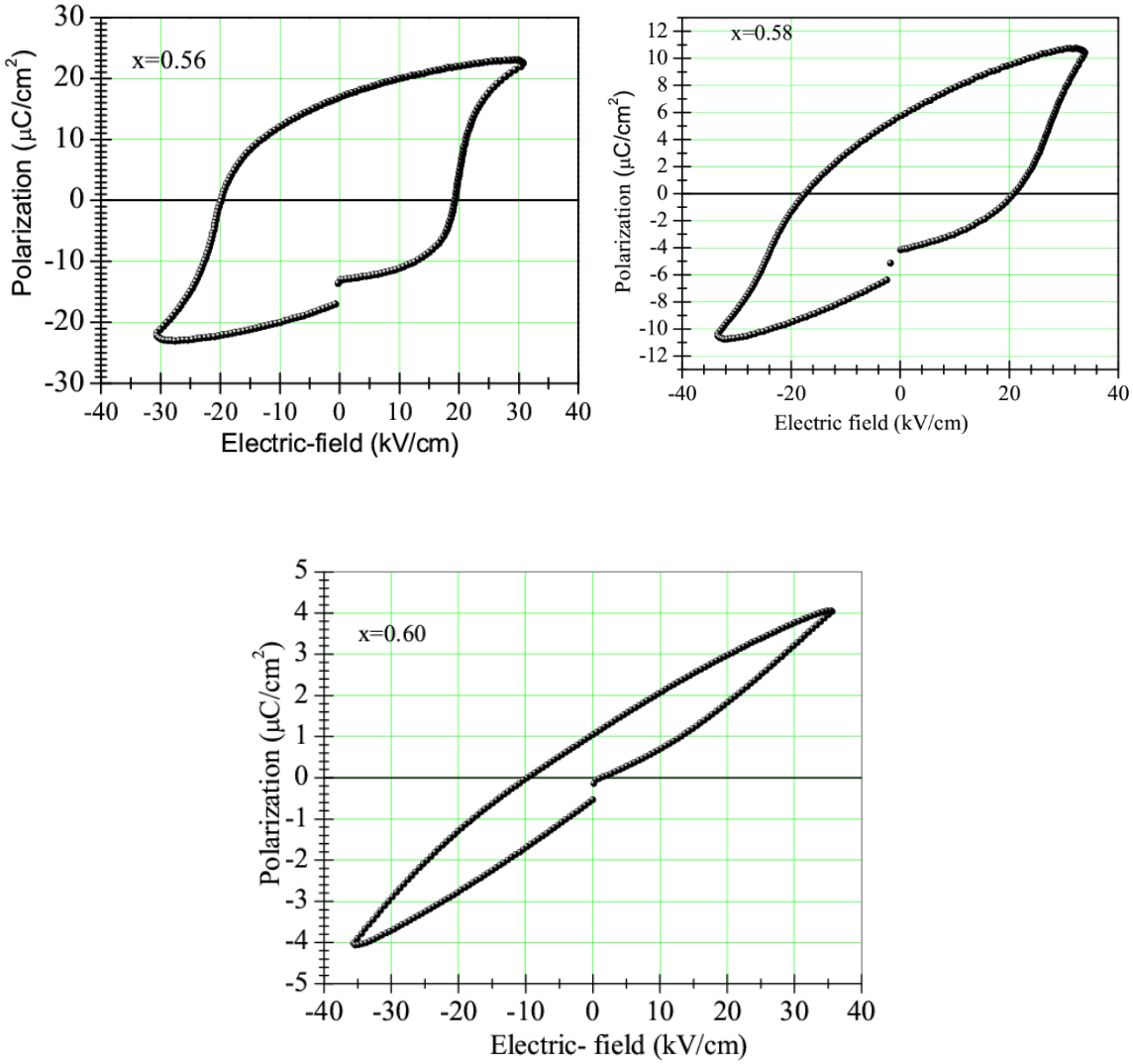


**Fig.4.17** P-E hysteresis loop for the BMZ-PT ceramics with (a) x=0.56, (b) x=0.58 and (c) x=0.60 recorded at 50Hz [Pandey et al (2014)].

Similarly, the hysteresis loop for the composition with x=0.58 showing the coexistence of the cubic and tetragonal phases is also less saturated than that for x=0.56. It seems that the reorientation of the nanodomains in x=0.56 occurs much more easily than the microscopic domains in x=0.60, preventing the saturation of the hysteresis loop. We tried to open the loop at higher electric fields but dielectric breakdown occurred. Below the Vogel Fulcher freezing temperature the nonergodic relaxor nature is observed in case of well-known $Pb(Mg_{1/3}Nb_{2/3})O_3$ where the domain switching and polarization saturation are possible under the electric field [Viehland et al. (1991)]. The ferroelectric phase stabilizes for the low temperature under electric field in case of $Pb(Mg_{1/3}Nb_{2/3})O_3$ system [Colla et al. (1995)].

To understand the observation of unsaturated hysteresis loop in tetragonal and two phase compositions we studied Polarization (P) - electric field (E) hysteresis loops with varying temperature for the compositions with x=0.55, 0.58, and 0.60 (see Fig.4.18). It can be seen from Fig.4.18(a), for x=0.55, the coercive field as well as polarization decreases with increasing temperature, as expected for ferroelectric materials. Very slim hysteresis loop is obtained at 130$^o$C. The inset of the Fig.4.18(a) shows the enlarged loop at 130$^o$C. With rising temperature, the tetragonal phase induced in cubic composition after poling, transforms again into cubic phase thereby decreasing the polarization. In case of two phase MPB composition with x=0.58, the polarization increases but the coercive field decreases as we increase the temperature (see Fig.4.18(b)). Since there is already a coexisting tetragonal phase at room temperature in x=0.58,

increasing temperature enhances the domain mobility which reduces coercive field and results in better alignment of the dipoles with higher polarization. In case of pure tetragonal composition with x=0.60 also, the polarization increases with increasing temperature as shown in Fig.4.18(c). Since at room temperature hysteresis loop is not open for x=0.60, it is not possible to get the value of coercive field at temperatures close to room temperature. Increasing temperature will enable the pinned ferroelectric domains to become mobile so that ferroelectric loop opens for x=0.60. At significantly higher temperature, in the proximity of the tetragonal to cubic phase transition, the tetragonality will start decreasing and will decrease the polarization as observed for x=0.55. We could not measure the P-E loops at further higher temperatures due to limitation of the experimental set-up. Large coercive field is reported for many other Bi-based solid solutions also [Maqbool et al. (2014) and references therein]. It has been shown for (1-x)$Bi_{1/2}Na_{1/2}TiO_3$-x$SrZrO_3$ solid solution that coercive field can be reduced very effectively by increasing the $SrZrO_3$ concentration as well as by increasing the temperature [Maqbool et al. (2014)].

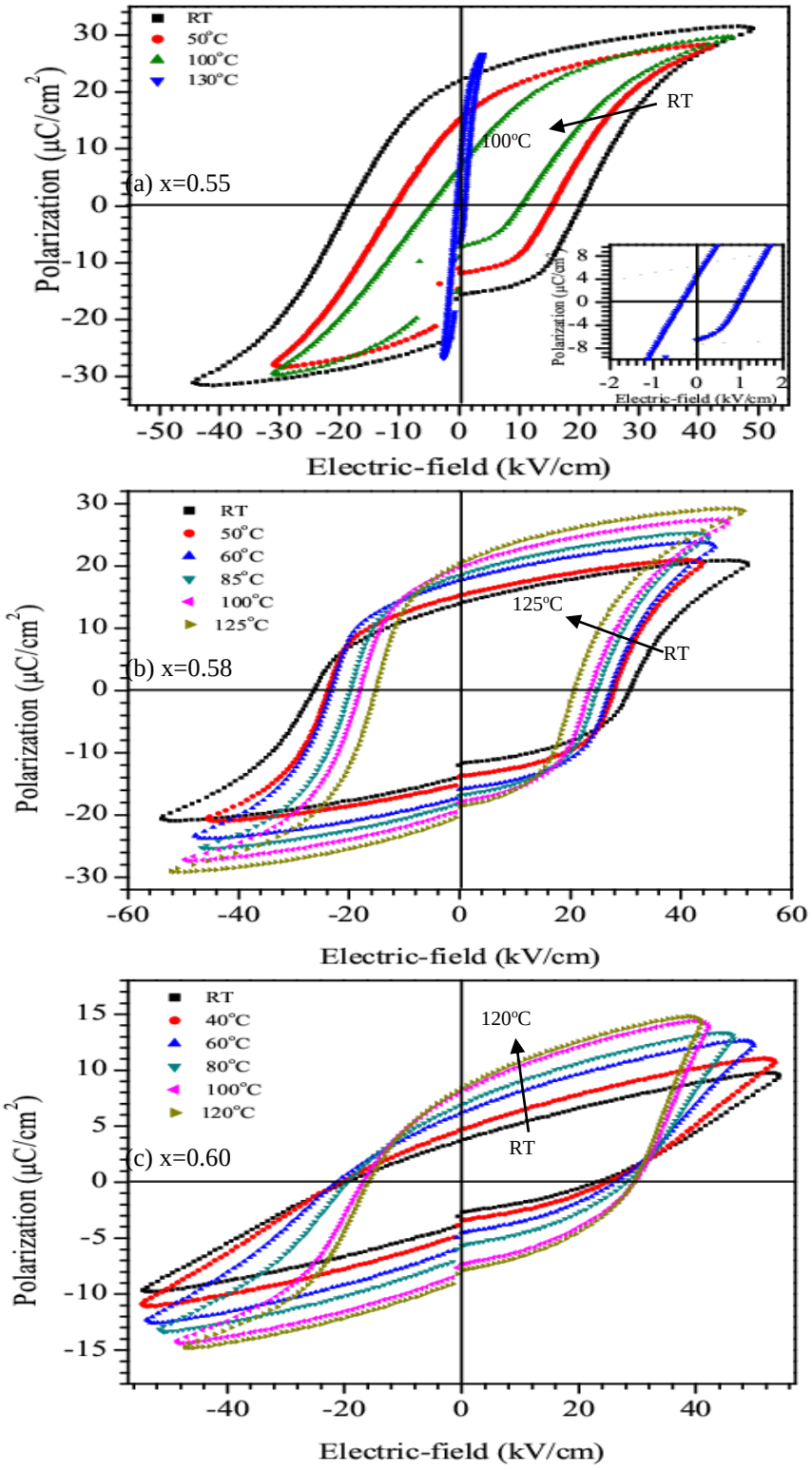


**Fig.4.18** Temperature dependent Polarization (P)- electric field (E) hysteresis loops of unpoled BMZ-PT piezoceramics with the compositions (a) x=0.55, (b) x=0.58 and (c) x=0.60.

## 4.5 Discussions

Crystallographic structure of MPB solid solution is very sensitive across MPB and may get modified by changing composition, temperature, electric field, stress, pressure etc. The electric field induced structural transformations have very crucial role on the piezoelectric response and have been investigated in several Bi-based solid solutions recently [Lee et al. (2011); Rao et al. (2013); Pandey et al. (2014); Royles et al. (2010); Simons et al. (2011); Zhao et al. (2014); Ma et al. (2012); Daniels et al. (2012)]. The pseudocubic composition of $(1-x)Bi(Ni_{1/2}Ti_{1/2})O_3$-$xPbTiO_3$ transforms to monoclinic phase in Pm space group after electric field poling [Pandey et al. (2014)]. Very high c-axis lattice strain is obtained due to the electric field induced phase transformation. In the $(1-x)Bi_{1/2}Na_{1/2}TiO_3$-$xBaTiO_3$ it is shown that the compositional width of the MPB can be irreversibly created/modified or destroyed by the application of poling field which can significantly affect the associated piezoelectric response [Ma et al. (2012)]. Daniel et al. (2012) have reported that for $0.93(Bi_{1/2}Na_{1/2})TiO_3$-$0.07BaTiO_3$ the grains with pseudocubic symmetry transform to tetragonal symmetry on applying the electric field and the c-axis preferentially aligns as close as possible to the applied electric field. Wang et al. (2014) reported that in case of polycrystalline $BaTiO_3$ the paraelectric cubic phase transforms to ferroelectric tetragonal phase above the Curie temperature under applied electric field. The application of electric field on lead zirconate titanate revealed an increase of the monoclinic phase fraction [Hinterstein et al. (2014)]. Many other lead based morphotropic phase boundary solid solutions are also reported to

show electric field induced structural changes and its significant role on the piezoelectric response close to the MPB [Zheng et al. (2015); Xu et al. (2008); Kovacova et al. (2014)].

The electric field induced transformation for BMT-PT from short range monoclinic (Pm) phase to long range monoclinic (space group Pm) phase in the composition with x=0.28 is accompanied by large c-axis lattice strain ~1.53%. This can be exploited for the piezoelectric actuator applications. However, eventhough in poled samples the largest saturation polarization is achieved in the pseudocubic composition with x=0.28, the maximum piezoelectric response is obtained around the composition with x=0.37 at the MPB [Randall et al. (2004); Upadhyay et al. (2015); Zhang et al. (2010)]. Fu and Cohen (2000) have reported that for a monoclinic structure the polarization vector has more freedom to rotate in response to applied electric field or stress and can lead to large piezoelectric response. In PZT [Singh et al. (2008)], PMN-PT [Singh et al. (2003); Ye et al. (2001)] and PZN-PT [Noheda et al. (2001)], it is reported that monoclinic structure acts as bridging phase between rhombohedral and tetragonal phases via which the polarization vector can continuously rotate under applied electric field stress and can result in large piezoelectric response. Contrary to that our present observation suggests that though the largest polarization is obtained for the composition (x=0.28) with monoclinic structure, the highest piezoelectric response is observed for the composition with coexisting tetragonal and monoclinic phases. The answer of this unusual observation lies in the switching behaviour of ferroelectric domains. It is well known that under applied electric

field or stress ferroelectric materials change the direction of polarization amongst crystallographically equivalent polarization directions by domain switching. For a single crystal there is no constraint to the domain switching under external stimulus but in polycrystalline ceramic materials domain switching in one grain is constrained by differently oriented polarization direction in the neighbouring grains. Li et al. (2005) have recently reported that in polycrystalline ceramics domain switching is difficult for the single phase tetragonal or rhombohedral/monoclinic structures whereas when two crystallographic symmetries coexist domain switching is significantly eased. In situ time resolved neutron diffraction studies by Jones et al. (2012) reveals that the cumulative piezoelectric response of the two phase MPB composition has the contributions from domain wall motion in both the tetragonal and monoclinic phases, interphase boundary motion between the two phases and electric field induced lattice strain. Domain wall motion is shown to give maximum contribution to piezoelectric response [Jones et al. (2012)]. In light of the observations of Li et al. (2005), the domain wall motion is expected to be maximum in the MPB composition of BMT-PT with x=0.37 when two phases coexist. The single phase monoclinic structure in x=0.28 gives lower piezoelectric response eventhough the electric field induced lattice strain is maximum for this composition. Further for the composition with x=0.37 one can also expect presence of electric field induced critical point close the tetragonal-monoclinic-cubic phase instability leading to higher piezoelectric response [Kutnjak et al. (2007)]. Thus present study reveals that the presence of mere monoclinic phase with more freedom for

polarization rotation is not enough for appearance of large piezoelectric response. Lattice instability in the vicinity of the critical point in the phase diagram and domain wall mobility are also key factors in deciding the piezoelectric response in MPB ceramics.

In case of BMZ-PT the composition with x=0.55 exhibits strong relaxor features in the temperature variation of permittivity [Pandey et al. (2014)]. Presence of Mg/Ti/Zr ions at B-site and Bi/Pb ions at A-site generates random electric field preventing development of long range ferroelectric order. This leads to pseudocubic symmetry for this composition. Electric field poling helps in override the random fields and results into long range tetragonal structure in this composition. Similar to our results, Royles et al. (2010) have reported that pseudocubic/rhombohedral phase of $0.2K_{1/2}Bi_{1/2}TiO_3$-$0.8Na_{1/2}Bi_{1/2}TiO_3$ transforms to a mixture of rhombohedral and tetragonal phases by application of electric field strength ≥20 kV/cm. This mixed phase persists even after removal of the electric field. Significant domain switching and large c-axis strain is reported to be associated with this phase transition.

## 4.6 Conclusions

We have investigated electric field induced structural transformations in several compositions of BMT-PT across MPB to correlate the structural changes after poling with the observed polarization and piezoelectric response. The pseudocubic composition with x=0.28, having short range monoclinic structure in the Pm space group is shown to exhibit isostructural transformation into long range monoclinic phase in the Pm space group. The structural transformation is

associated with large c-axis lattice strain of 1.53%. The tetragonal compositions with x=0.38 and 0.40 exhibit significant domain extension and reorientation along c-axis. The composition with x=0.35 having coexisting tetragonal and monoclinic phases shows change in the relative phase fraction of the two phases and significant domain extension and reorientation along the c-axis for both the tetragonal and monoclinic phases. The polarization-electric field hysteresis measurements on the unpoled samples show unsaturated hysteresis loops for all the compositions investigated. After poling well saturated hysteresis loop is observed for all the composition with maximum polarization for the composition with x=0.28 having single phase monoclinic structure in the Pm space group. Apart from the monoclinic symmetry the contributions from domain wall mobility has crucial role to give larger piezoelectric response for the MPB composition with x=0.37.

Electric field induced structural phase transition in polycrystalline BMZ-PT piezoceramics is observed for MPB and pseudocubic compositions close to MPB. The tetragonal composition (x=0.61) shows domain reorientation and domain extension only after electric field poling. The composition with x=0.55 having pseudocubic structure (space group Pm3m) at room temperature transforms to a phase mixture of tetragonal (space group P4mm) and cubic (space group Pm3m) structures after poling. The MPB composition (x=0.58) shows change in relative proportion of the two coexisting phases and large c-axis strain in tetragonal phase after poling. Appearance of well saturated hysteresis loop in pseudocubic composition is linked with an electric field induced phase transition.

Unsaturated hysteresis loops observed in tetragonal and MPB compositions are due to large coercive field.